Available online at www.sciencedirect.com
ScienceDirect
Journal of Sound and Vibration 298 (2006) 307–318
JOURNAL OF SOUND AND VIBRATION
www.elsevier.com/locate/jsvi

Stability of a spinning disk under a stationary oscillating unit

T.H. Young*, C.Y. Lin

Department of Mechanical Engineering, National Taiwan University of Science and Technology, 43 Section 4, Keelung Road, Taipei, 106, Taiwan

Received 23 May 2005; received in revised form 10 May 2006; accepted 22 May 2006
Available online 2 August 2006

Abstract

The free vibration and elastic stability of a spinning annular plate transversely in contact with a stationary oscillating unit is studied in this paper. The oscillating unit consists of two parallel combinations of springs and dampers attached above and under a mass. Therefore, the displacement of the mass is not the same as that of the disk at the contact point. In this work, the equations of motion of the spinning disk and the oscillating unit in an inertial coordinate system are given first, and the displacement of the disk is expressed in terms of the eigenfunctions of the stationary disk. The Galerkin method is then applied to obtain the discretized system equations for the disk, and these equations are combined with the equation for the oscillating unit. Finally, the stability analysis is conducted by investigating the eigenvalue problem of the combined system. Numerical results show that taking account of the stiffness between the oscillating unit and the disk may bring about extra flutter-type instability between the predominantly oscillating-unit mode and the predominantly reflected disk modes, and these extra unstable regions are much larger than those of the flutter-type instability between different kinds of predominantly disk modes.

1. Introduction

Spinning disks are widely used components in mechanical engineering from circular saw blades, turbine rotors to computer disk memory units. Therefore, the dynamic behaviors of spinning disks have attracted researchers' interest for a long time. Early works on the vibration of spinning disks dealt primarily with the determination of the natural frequencies and the mode shapes of the disks [1–3] and with the nonlinear response of the disk due to large amplitude vibration [4,5].

For computer disk memory units, the interaction of the read/write head with the surface of the disk demands that the effects of the inertia, stiffness and damping of the head be considered in the analysis. To minimize the complication of the problem due to the rotational inertia effect of the disk, Iwan and stahl [6] first studied the free vibration and stability of a stationary circular disk excited by a rotating mass-spring–damper load system. The displacement of the mass of the load system is assumed to be equal to the transverse deflection of the disk. Three distinct types of instability are observed in this paper. A region of the divergence type of instability occurs immediately above each critical speed of the disk. Some regions of the

*Corresponding author. Tel.: 886 2 27376444; fax: 886 2 27376460.
E-mail address: thyoung@mail.ntust.edu.tw (T.H. Young).

0022-460X/$ - see front matter © 2006 Elsevier Ltd. All rights reserved.
doi:10.1016/j.jsv.2006.05.024

flutter type of instability arise as a consequence of modal interaction of the disk. A region of the flutter type of instability between a reflected mode and its forward mode, the so-called terminal instability, exists for all load speeds above a certain limiting value. Later Iwan and Moeller [7] included the rotational inertia effect of the disk and investigated the free vibration and stability of a spinning disk with a stationary mass-spring–damper load system. They found that the primary effect of the disk rotation was to stiffen the disk and thereby increase effective natural frequencies over those of a stationary disk with a rotating load system. Furthermore, the analysis indicates that the width of the region of the divergence type of instability is a function of the load stiffness and radius but not of the load mass, and the location of the terminal instability region is a strong function of the load mass and radius but only a weak function of the load stiffness.

Ono et al. [8] extended Iwan and Moeller's work to include the corresponding pitching parameters in the load system and the friction force between the spinning disk and the stationary load system. They found that the pitching parameters have similar effects as their transverse counterparts, and the friction force tends to destabilize the forward traveling waves but stabilize the reflected and backward traveling waves. Chen and Bogy [9,10] studied the effects of load parameters and modal interaction on the natural frequencies and stability of a spinning disk with a stationary load system. They concluded that adding a small mass (weak spring) in the load system tends to decrease (increase) the natural frequencies of the forward and backward traveling waves but tends to increase (decrease) the natural frequencies of the reflected traveling waves; adding a small damper in the load system tends to stabilize the forward and backward traveling waves but destabilize the reflected traveling waves.

For circular saws, the blade is often restrained from lateral motion during cutting by guide pads to minimize the vibration of the blade. Hutton et al. [11] analyzed the dynamic response of a rotating disk subjected to excitations produced by stationary point loads and restrained by stationary point springs. A general approach to investigate the instability phenomena due to the interaction between a rotating disk and an interactive stationary system was developed by Tian and Hutton [12]. Shen and Mote [13–15] presented a series of studies on parametric instability of stationary circular plates under a rotating mass and of stationary circular plates with inclusions under a spring or a mass-spring–dashpot system.

In the above-mentioned references, the displacement of the mass of the load system is assumed to be the same as that of the disk at the contact point. In reality, the displacement of the mass of the load system may not be the same as that of the disk. Therefore, this work investigates the free vibration and elastic stability of a spinning annular plate transversely in contact with a stationary oscillating unit. The oscillating unit consists of two parallel combinations of springs and dampers attached above and under a mass such that the displacement of the mass is not the same as that of the disk at the contact point.

2. Formulation

Consider an annular plate that is clamped at the inner edge $r = a$ and is free at the outer edge $r = b$, where (r,θ) is a polar coordinate system fixed in space. The disk is spinning at an angular speed Ω and is transversely in contact with a stationary oscillating unit at the point $(r_P,0)$. The oscillating unit consists of two parallel combinations of springs and dampers attached above and under a mass. The lower end of the oscillating unit is assumed to contact with the plate closely, and the upper end of it is fastened to a fixed support, as shown in Fig. 1.

With respect to the inertial polar coordinates, the transverse displacement of the plate can be expressed as $w = w(r,\theta(t),t)$. Therefore, the equation of motion of a spinning disk with viscous damping under the action of the stationary oscillating unit is written as

$$D\nabla^4 w + c\left(\frac{\partial w}{\partial t} + \Omega\frac{\partial w}{\partial \theta}\right) + \rho h\left(\frac{\partial^2 w}{\partial t^2} + 2\Omega\frac{\partial^2 w}{\partial t\partial\theta} + \Omega^2\frac{\partial^2 w}{\partial\theta^2}\right) = h\left[\frac{1}{r}\frac{\partial}{\partial r}\left(r\sigma_{rr}\frac{\partial w}{\partial r}\right) + \frac{1}{r^2}\sigma_{\theta\theta}\frac{\partial^2 w}{\partial\theta^2}\right] + \frac{P}{r_P}\delta(r - r_P)\delta(\theta), \quad (1)$$

where D and c are the flexural rigidity and viscous damping coefficient of the disk, respectively; ρ and h are the mass density and thickness of the disk, respectively; ∇^4 is a biharmonic operator, and $\delta(\cdot)$ is a Dirac delta

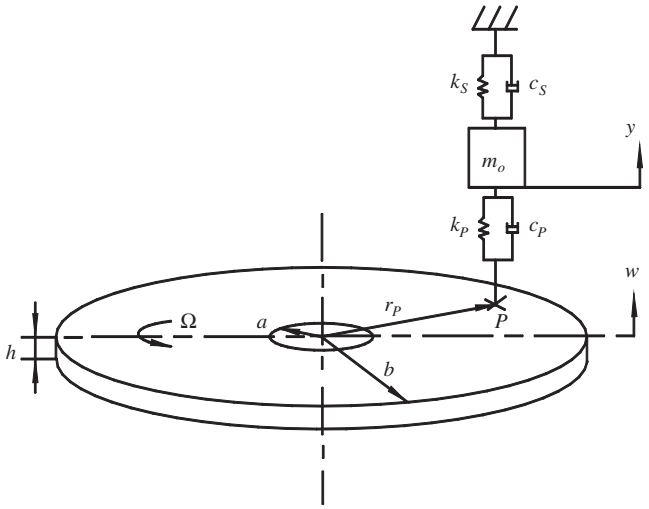

Fig. 1. A spinning disk under a stationary oscillating unit.

function. The force acted upon the disk by the oscillating unit P is

$$P = c_P\dot{y} + k_P y, \tag{2}$$

where y is the relative displacement of the mass of the oscillating unit, and an overdot denotes a differentiation with respect to time t. The initial in-plane stresses induced by rotation σ_{rr} and $\sigma_{\theta\theta}$ are found to be [16]

$$\sigma_{rr} = d_0 + d_1\left(\frac{a}{r}\right)^2 + d_2\left(\frac{r}{a}\right)^2,$$
$$\sigma_{\theta\theta} = d_0 - d_1\left(\frac{a}{r}\right)^2 + d_3\left(\frac{r}{a}\right)^2 \tag{3}$$

in which the constants are given by

$$d_0 = \frac{1+v}{8}\frac{[(1-v)a^4 + (3+v)b^4]}{(1-v)a^2 + (1+v)b^2}\rho\Omega^2, \quad d_2 = -\frac{(3+v)a^2}{8}\rho\Omega^2,$$

$$d_1 = \frac{1-v}{8}\frac{[(3+v)b^2 - (1+v)a^2]b^2}{(1-v)a^2 + (1+v)b^2}\rho\Omega^2, \quad d_3 = -\frac{(1+3v)a^2}{8}\rho\Omega^2,$$

where v is Poisson's ratio of the disk. The boundary conditions of the disk in terms of the transverse displacement are

$$w = \frac{\partial w}{\partial r} = 0, \quad \text{at } r = a,$$

$$\frac{\partial^2 w}{\partial r^2} + v\left(\frac{1}{r}\frac{\partial w}{\partial r} + \frac{1}{r^2}\frac{\partial^2 w}{\partial \theta^2}\right) = 0, \quad \text{at } r = b,$$

$$\frac{\partial}{\partial r}\left(\frac{\partial^2 w}{\partial r^2} + \frac{1}{r}\frac{\partial w}{\partial r} + \frac{1}{r^2}\frac{\partial^2 w}{\partial \theta^2}\right) + \frac{1-v}{r^2}\left(\frac{\partial^3 w}{\partial r \partial \theta^2} - \frac{1}{r}\frac{\partial^2 w}{\partial \theta^2}\right) = 0. \tag{4}$$

The equation of motion of the oscillating unit is given by

$$m_o\ddot{y} + (c_S + c_P)\dot{y} + (k_S + k_P)y = -m_o\frac{\partial^2 w}{\partial t^2}(r_P, 0, t) - c_S\frac{\partial w}{\partial t}(r_P, 0, t) - k_S w(r_P, 0, t). \tag{5}$$

Therefore, the force acted upon the disk by the oscillating unit can be rewritten as

$$P = -m_o\left[\ddot{y} + \frac{\partial^2 w}{\partial t^2}(r_P, 0, t)\right] - c_S\left[\dot{y} + \frac{\partial w}{\partial t}(r_P, 0, t)\right] - k_S[y + w(r_P, 0, t)]. \tag{6}$$

Eq. (1) is a partial differential equation in spatial coordinates and time, while Eq. (5) is an ordinary differential equation in time. These two equations are coupled and are very difficult to solve for the exact solution. Therefore, an approximate method is utilized to eliminate the dependence of the transverse displacement of the disk on the spatial coordinates. In this work, the Galerkin method is adopted to discretize the equation of motion of the spinning disk. Assume that the solution of Eq. (1) can be expressed as a linear combination of the eigenfunctions of the corresponding stationary disk, that is

$$w(r, \theta, t) = \sum_{m=0}^{M}\sum_{n=0}^{N} R_{mn}(r)[A_{mn}(t)\cos n\theta + B_{mn}(t)\sin n\theta], \tag{7}$$

where $R_{mn}(r)$ is a combination of Bessel functions such that the displacement in Eq. (7) satisfies the boundary conditions of the disk. Substituting Eq. (7) into Eq. (1), going through Galerkin's procedure and combining Eq. (6) yields the discretized equations for the whole system—the spinning disk and the oscillating unit,

$$[M]\mathbf{a}'' + \left(2\alpha\bar{\Omega}[C] + 2\bar{\Omega}[G]\right)\mathbf{a}' + \left([K^e] + \bar{\Omega}^2[K^r] + 2\alpha\bar{\Omega}^2[G]\right)\mathbf{a} = \mathbf{0}, \tag{8}$$

where $\bar{\Omega} = \sqrt{\rho h b^4/D}\Omega$ and $\alpha = c/2\rho h\Omega$; $[M]$, $[C]$ and $[G]$ are the mass, damping and gyroscopic matrices of the whole system, respectively; $[K^e]$ and $[K^r]$ are the elastic stiffness matrix and the geometric stiffness matrix due to rotation, respectively; $\mathbf{a}$ is a column matrix formed by all A_{mn}, B_{mn} and y, and a prime denotes a differentiation with respect to the dimensionless temporal variable $\tau = t\sqrt{D/\rho h b^4}$.

Eq. (8) is a set of the second-order ordinary differential equations in time, and it can be rewritten into a set of the first-order differential equations as

$$\left(\begin{bmatrix}[M] & [0]\\ [0] & [I]\end{bmatrix}\right)\mathbf{q}' + \left(\begin{bmatrix}2\alpha\bar{\Omega}[C] + 2\bar{\Omega}[G] & [K^t] + 2\alpha\bar{\Omega}^2[G]\\ -[I] & [0]\end{bmatrix}\right)\mathbf{q} = \mathbf{0}, \tag{9}$$

where $[I]$ is an identity matrix; $[K^t] = [K^e] + \bar{\Omega}^2[K^r]$ and $\mathbf{q} = \begin{bmatrix}\mathbf{a}'\\ \mathbf{a}\end{bmatrix}$. The solution of Eq. (9) has the form

$$\mathbf{q} = \mathbf{x}e^{\lambda\tau}, \tag{10}$$

where λ is a constant scalar, and $\mathbf{x}$ is a constant vector. Introducing Eq. (10) into Eq. (9) and dividing both sides by $e^{\lambda\tau}$ yields the following eigenvalue problem:

$$\lambda\left(\begin{bmatrix}[M] & [0]\\ [0] & [I]\end{bmatrix}\right)\mathbf{x} + \left(\begin{bmatrix}2\alpha\bar{\Omega}[C] + 2\bar{\Omega}[G] & [K^t] + 2\alpha\bar{\Omega}^2[G]\\ -[I] & [0]\end{bmatrix}\right)\mathbf{x} = \mathbf{0}. \tag{11}$$

Because the matrices in Eq. (11) are asymmetric, both the eigenvalues and the eigenvectors of the problem appear in complex conjugate pairs, i.e., $\lambda = \xi \pm i\omega$ and $\mathbf{x} = \mathbf{y} \pm i\mathbf{z}$. When the real part of an eigenvalue ξ becomes positive, the corresponding mode is unstable. Furthermore, if the imaginary part of this eigenvalue ω is equal to 0, the corresponding mode experiences a divergence type of instability; if the imaginary part of this eigenvalue is not equal to 0, the corresponding mode experiences a flutter type of instability.

3. Numerical results and discussions

Before conducting the parametric studies of the system parameters on the stability of the whole system—the disk and the oscillating unit, a comparison of the present results with the existing references is made first. If the inner radius is assumed to approach zero, and the spring constant and viscous damping coefficient of the lower spring-damper combination are assumed to approach infinity such that the displacement of the mass is the same as that of the disk at the contact point, the problem considered in this work is reduced to that studied by Iwan and Moeller [7]. Fig. 2 shows the real and imaginary parts of the eigenvalues of the problem with a very

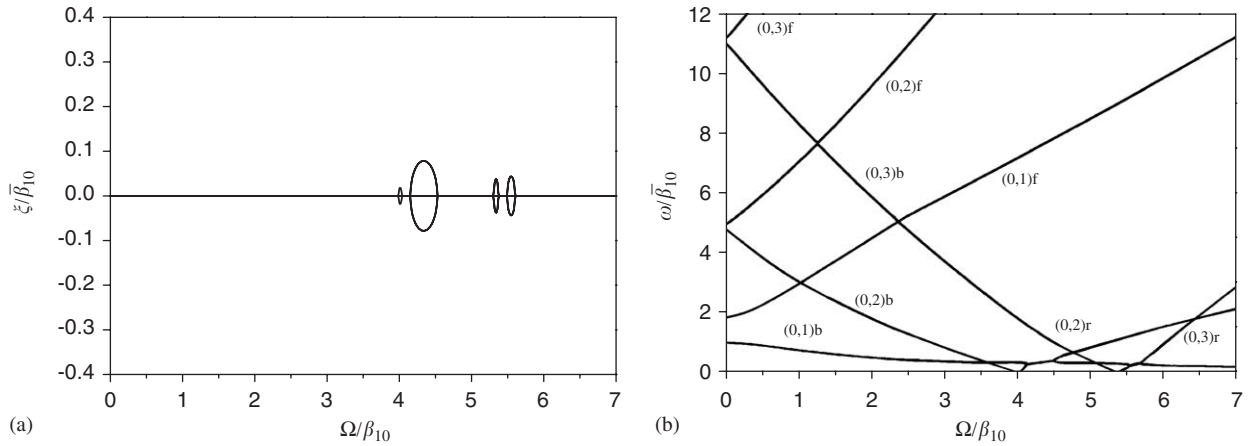

Fig. 2. The real and imaginary parts of the eigenvalues of a spinning disk under a stationary oscillating unit with an extremely stiff lower spring and damper. $v = 0.3$, $a/b = 10^{-6}$, $\bar{r}_P = 0.6$, $\bar{m}_o = 0.1$, $\bar{k}_P = \bar{c}_P = 10^{10}$, $\bar{k}_S = 4.0$, $\bar{c}_S = \bar{c} = 0$.

small inner-to-outer radius ratio and extremely large spring constant and viscous damping coefficient of the lower spring-damper combination. Fig. 2(a) shows the real parts of the eigenvalues; Fig. 2(b) shows the imaginary parts of the eigenvalues. The non-dimensionalized parameters used in this section are defined in the same way as those in Iwan and Moeller's paper, i.e., $\bar{m}_o = m_o/M$, $\bar{k}_P = k_P/M\beta_{10}^2$,

$$\bar{k}_S = k_S/M\beta_{10}^2, \quad \bar{c}_P = c_P/M\beta_{10}, \quad \bar{c}_S = c_S/M\beta_{10}, \quad \bar{c} = c/2\rho h\beta_{10},$$

where $M = \pi\rho h(b^2 - a^2)$ is the mass of the disk, and $\beta_{10} = 1.11805\sqrt{D/\rho h b^4}$ is the natural frequency of the zero nodal circle and one nodal diameter mode of the corresponding stationary disk. The predominantly forward traveling, backward traveling and reflected plate modes (simply called forward, backward and reflected modes hereafter) with m nodal circles and n nodal diameters are denoted as $(m,n)f$, $(m,n)b$ and $(m,n)r$, respectively. Fig. 2(a) reveals that except at four unstable intervals, the real parts of the eigenvalues are identically zero because the whole system considered here is undamped. Fig. 2(b) reveals that these four unstable intervals correspond to two divergence-type instability of the $(0,2)b$ and $(0,3)b$ modes as their frequency curves meet the coordinate axis, and two flutter-type instability by $(0,2)r$ and $(0,1)b$ modes and by $(0,3)r$ and $(0,1)b$ modes as their frequency curves intersect. The results agree excellently with those in Iwan and Moeller's paper.

By piling up the unstable intervals with respect to a certain parameter, stability boundaries of the whole system can be obtained. Fig. 3 presents the stability boundaries of a spinning annular disk subjected to a stationary oscillating unit with an extremely large spring constant and viscous damping coefficient of the lower spring–damper combination such that the displacement of the mass is the same as that of the disk at the contact point. In this figure, unstable regions are bounded within a pair of stability boundaries. Because of the space limitation, each unstable region is labeled by a letter instead of the modes involves, and the nomenclature of all symbols for unstable regions is listed in Table 1. The unstable regions of flutter-type instability by $(0,3)r$ and $(0,1)b$ modes, flutter-type instability by $(0,2)r$ and $(0,4)b$ modes and flutter-type instability by $(0,3)r$ and $(0,4)b$ modes are very close. All unstable regions are nearly unchanged with respect to changes of the mass of the oscillating unit.

The real and imaginary parts of the eigenvalues of a spinning annular disk subjected to a stationary oscillating unit are illustrated in Fig. 4. The spring constant of the lower spring is small so that the natural frequency of the oscillating unit is commensurable with the lowest few natural frequencies of the disk, and the lower damper is absent. Under this circumstance, the displacement of the mass is different from that of the disk at the contact point. Fig. 4(a) shows the real parts of the eigenvalues; Fig. 4(b) shows the imaginary parts of the eigenvalues. There is a horizontal dash line at ω around 3.5 in Fig. 4(b) representing the frequency line of the independent oscillating unit. The frequency line becomes a curve due to the interaction between the

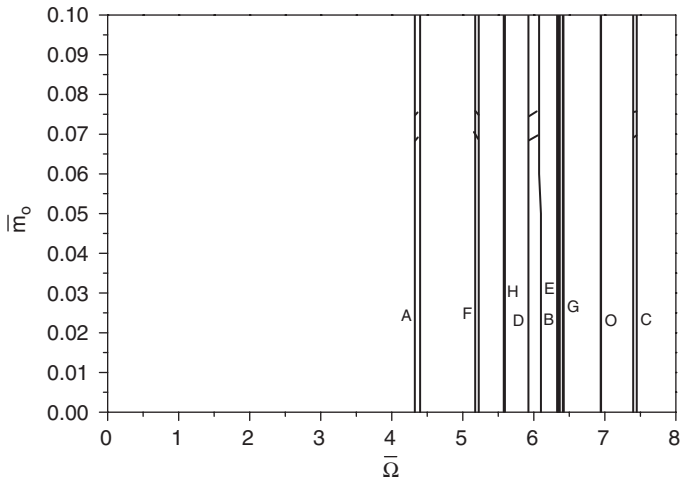

Fig. 3. The stability boundaries of a spinning disk under a stationary oscillating unit with an extremely stiff lower spring and damper. $v = 0.3$, $a/b = 0.1$, $\bar{r}_P = 0.7$, $\bar{k}_P = \bar{c}_P = 10^{10}$, $\bar{k}_S = 0.05$, $\bar{c}_S = \bar{c} = 0$.

Table 1
Nomenclature of symbols for unstable regions

Symbol	Instability type
A	Divergence-type instability due to the (0,2)b mode
B	Flutter-type instability between the (0,3)r and the (0,1)b modes
C	Flutter-type instability between the (0,4)r and the (0,1)b modes
D	Flutter-type instability between the (0,2)r and the (0,1)b modes
E	Flutter-type instability between the (0,2)r and the (0,4)b modes
F	Flutter-type instability between the (0,2)r and the (0,3)b modes
G	Flutter-type instability between the (0,3)r and the (0,4)b modes
H	Divergence-type instability due to the (0,3)b mode
I	Flutter-type instability between the (0,3)r and the (0,2)b modes
J	Flutter-type instability between the (0,4)r and the (0,3)b modes
K	Flutter-type instability between the (0,3)r and the oscillating-unit modes
L	Flutter-type instability between the (0,4)r and the oscillating-unit modes
M	Flutter-type instability between the (0,2)r and the oscillating-unit modes
N	Flutter-type instability between the (0,4)r and the (0,2)b modes
O	Divergence-type instability due to the (0,4)b mode

oscillating unit and the disk. Flutter-type instability occurs as this frequency curve intersects those of the reflected modes. The other small unstable intervals in Fig. 4(a) correspond to the divergence-type instability of the backward modes and the flutter-type instability by the reflected and backward modes. The stability boundaries of this problem are depicted in Fig. 5. The unstable regions of the divergence-type instability of the backward modes and the flutter-type instability by the reflected and backward modes are almost constant with respect to the mass ratio. But the unstable regions of the flutter-type instability between the predominantly oscillating-unit mode and the reflected modes lean toward the lower speed range because an increase in the mass will reduce the natural frequency of the oscillating unit. When the unstable region of the flutter-type instability by the $(0, 3)r$ and the predominantly oscillating-unit modes meets that of the flutter-type instability by the $(0, 4)r$ and the predominantly oscillating-unit modes at $\bar{m}_o$ around 0.03, these two unstable regions coalesce into one unstable region because they share a common mode—the predominantly oscillating-unit mode. The unstable regions of the flutter-type instability between the predominantly oscillating-unit mode and the reflected modes are much larger than those purely by the predominantly disk modes only. Furthermore,

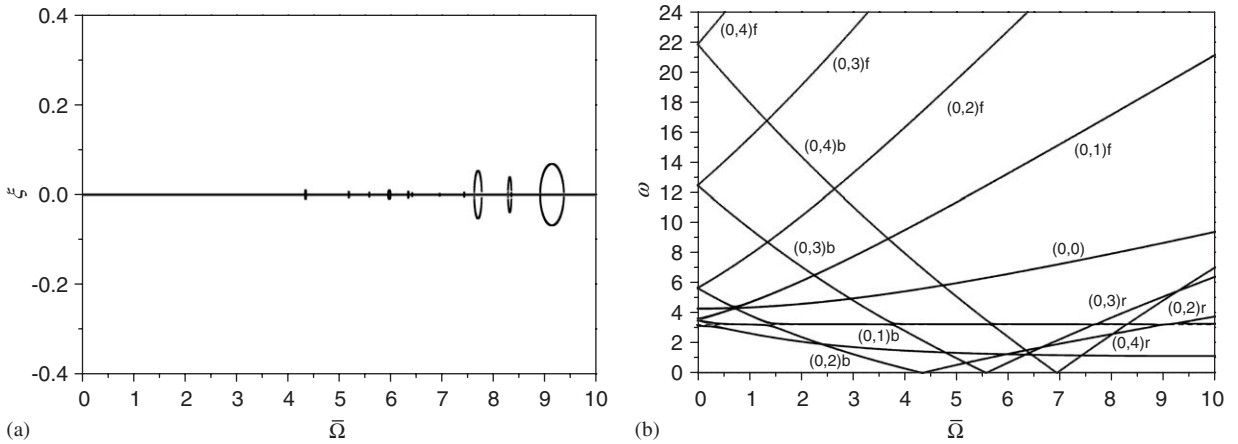

Fig. 4. The real and imaginary parts of the eigenvalues of a spinning disk under a stationary oscillating unit. $v = 0.3$, $a/b = 0.1$, $\bar{r}_P = 0.7$, $\bar{m}_o = 0.1$, $\bar{k}_P = 0.025$, $\bar{k}_S = 0.05$, $\bar{c}_P = \bar{c}_S = \bar{c} = 0$.

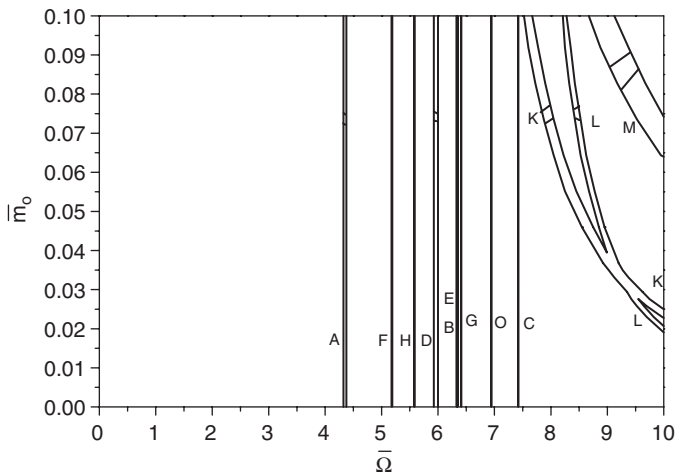

Fig. 5. The effect of the mass on the stability boundaries of a spinning disk under a stationary oscillating unit. $v = 0.3$, $a/b = 0.1$, $\bar{r}_P = 0.7$, $\bar{k}_P = 0.025$, $\bar{k}_S = 0.05$, $\bar{c}_P = \bar{c}_S = \bar{c} = 0$.

a comparison between Figs. 5 and 3 reveals that the unstable regions purely by the predominantly disk modes only become smaller. Therefore, inclusion of a spring between the disk and the mass of the oscillating unit will bring about new and larger unstable regions between the predominantly oscillating-unit mode and the reflected modes but repress the original instability purely by the predominantly disk modes only.

Fig. 6 shows the real and imaginary parts of the eigenvalues of a spinning annular disk subjected to a stationary oscillating unit with a stiffer lower spring. Fig. 6(a) shows the real parts of the eigenvalues, and there are four small and one large unstable intervals. Fig. 6(b) shows the imaginary parts of the eigenvalues, and the dash line and curves are the frequency line of the oscillating unit alone and the frequency curves of the free spinning disk, respectively. Due to the interaction between the oscillating unit and the disk, the frequency line of the oscillating unit becomes a tortuous curve, and the frequency curves of the disk near the frequency line of the oscillating unit become zigzag. Away from this frequency line, the frequency curves of the disk are basically unaffected. The four small unstable intervals are formed by the divergence- or flutter-type instability of the predominantly disk modes, while the large unstable interval is formed by two flutter-type instability between the predominantly oscillating-unit mode and the reflected modes connecting together. Fig. 7 presents the stability boundaries of the whole system versus the spring constant of the lower spring. The unstable region of the flutter-type instability by the $(0,2)r$ and $(0,4)b$ modes lies inside the unstable region of the

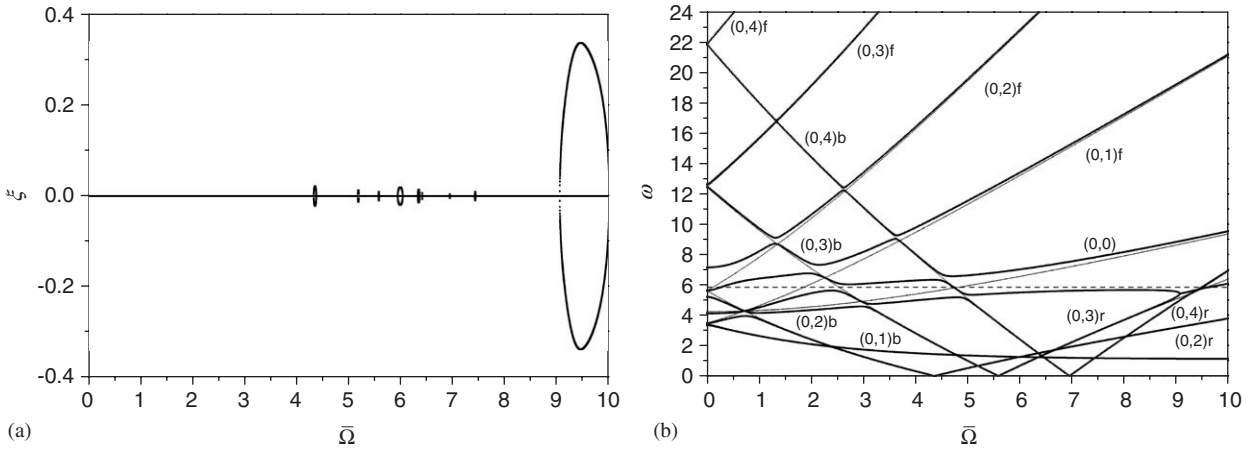

Fig. 6. The real and imaginary parts of the eigenvalues of a spinning disk under a stationary oscillating unit. $v = 0.3$, $a/b = 0.1$, $\bar{r}_P = 0.7$, $\bar{m}_o = 0.1$, $\bar{k}_P = 0.2$, $\bar{k}_S = 0.05$, $\bar{c}_P = \bar{c}_S = \bar{c} = 0$.

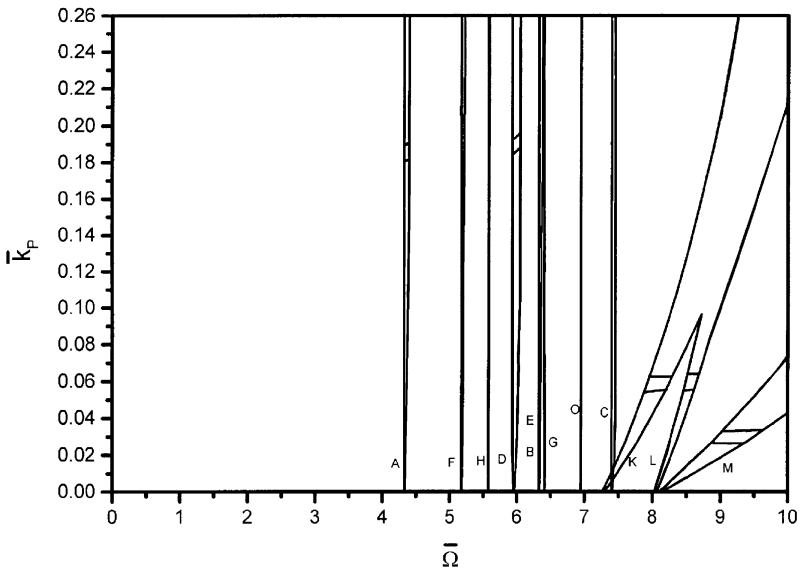

Fig. 7. The effect of the lower spring on the stability boundaries of a spinning disk under a stationary oscillating unit. $v = 0.3$, $a/b = 0.1$, $\bar{r}_P = 0.7$, $\bar{m}_o = 0.1$, $\bar{k}_S = 0.05$, $\bar{c}_P = \bar{c}_S = \bar{c} = 0$.

flutter- type instability of the $(0, 3)r$ and $(0, 1)b$ modes. The widths of the unstable regions of the predominantly disk modes widen as $\bar{k}_P$ increases, but the locations of these unstable regions stay at the same positions. The unstable region of the flutter-type instability between the $(0, 3)r$ and the predominantly oscillating-unit modes and the unstable region of the flutter-type instability between the $(0, 4)r$ and the predominantly oscillating-unit modes coalesce as they meet at $\bar{k}_P$ around 0.095. As $\bar{k}_P$ increases, the unstable regions of the flutter-type instability between the reflected modes and the predominantly oscillating-unit mode enlarge and lean toward the higher speed range because an increase in $\bar{k}_P$ will raise the natural frequency of the oscillating unit. The effect of the upper spring is similar to that of the lower spring.

Fig. 8 shows the stability boundaries of a spinning annular disk with a larger inner-to-outer radius ratio subjected to a stationary oscillating unit. In this figure, the unstable region of the flutter-type instability between the $(0, 3)r$ and the predominantly oscillating-unit modes crosses over the unstable region of

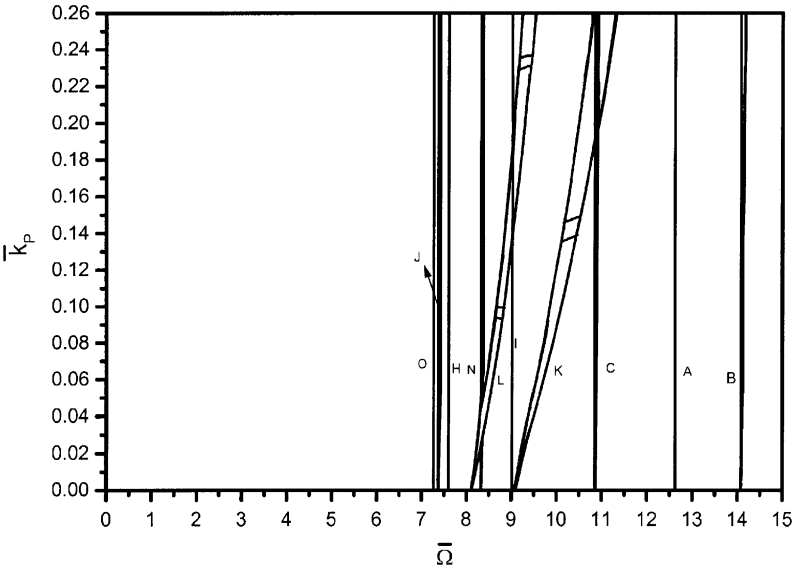

Fig. 8. The stability boundaries of a spinning disk with a larger inner-to-outer radius ratio under a stationary oscillating unit. $v = 0.3$, $a/b = 0.5$, $\bar{r}_P = 0.7$, $\bar{m}_o = 0.1$, $\bar{k}_S = 0.05$, $\bar{c}_P = \bar{c}_S = \bar{c} = 0$.

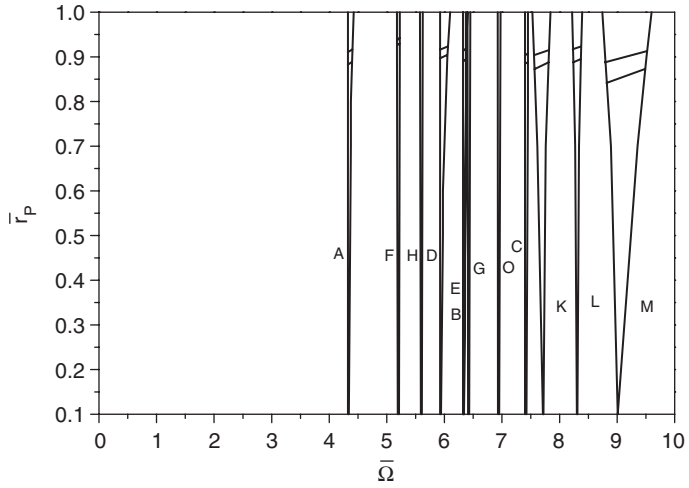

Fig. 9. The effect of the location of the oscillating unit on the stability boundaries of a spinning disk under a stationary oscillating unit. $v = 0.3$, $a/b = 0.1$, $\bar{m}_o = 0.1$, $\bar{k}_P = 0.025$, $\bar{k}_S = 0.05$, $\bar{c}_P = \bar{c}_S = \bar{c} = 0$.

the flutter- type instability between the $(0,4)r$ and $(0,1)b$ modes, but these two unstable regions do not merge into one unstable region because they do not have a common mode involved. A comparison with Fig. 7 shows that the unstable regions in this figure are either different from those in Fig. 7 or at different locations for the same instability. The reason is that the frequency curves of the disk change quite a lot for different inner-to-outer radius ratios. The unstable regions in this figure are much smaller than those in Fig. 7 because for the same outer radius, a larger inner radius stands for a stiffer disk. Therefore, a larger inner-to-outer radius ratio is favorable to the stability of the whole system.

Fig. 9 illustrates the stability boundaries of the whole system versus the location of the oscillating unit. All the unstable regions, no matter the instability by the predominantly disk modes only or the instability between the reflected modes and the predominantly oscillating-unit mode, enlarge as $\bar{r}_P$ increases. This may be attributed to the fact that a longer distance between the contact point and the disk center will increase the

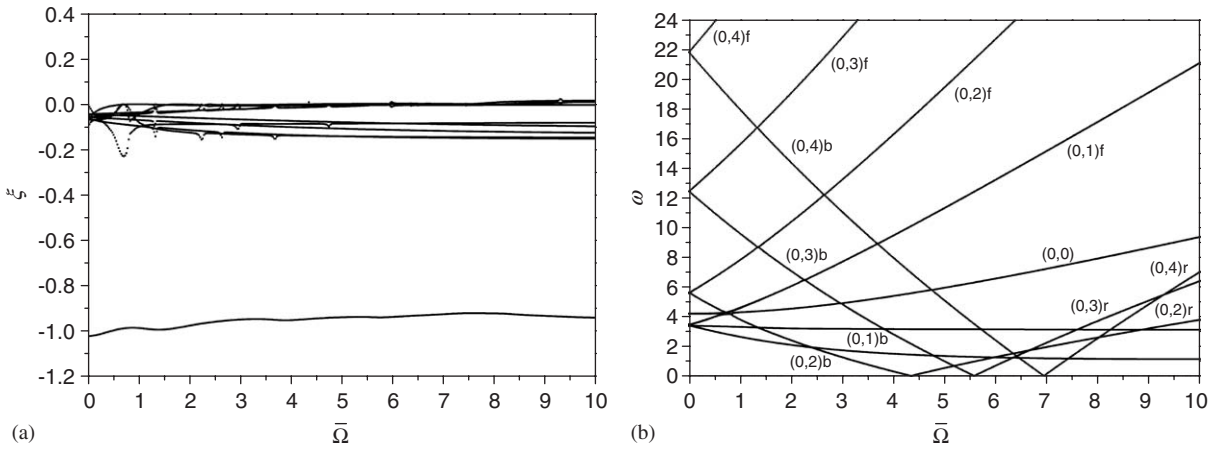

Fig. 10. The effect of the lower damper on the eigenvalues of a spinning disk under a stationary oscillating unit. $v = 0.3$, $a/b = 0.1$, $\bar{r}_P = 0.7$, $\bar{m}_o = 0.1$, $\bar{k}_P = 0.025$, $\bar{k}_S = 0.05$, $\bar{c}_P = 0.05$, $\bar{c}_S = \bar{c} = 0$.

bending moment of the disk produced by the action of the oscillating unit. Therefore, the effect of the location of the oscillating unit is destabilizing when it is moved towards the rim of the disk.

The effect of the lower damper of the oscillating unit on the eigenvalues of the whole system is shown in Fig. 10. Fig. 10(a) shows the real parts of the eigenvalues. The single curve at the lower side of the figure belongs to the predominantly oscillating-unit mode, and the other curves near the horizontal coordinate axis belong to the predominantly disk modes. One of these curves crosses the horizontal coordinate axis at $\bar{\Omega} = 4.35$, which is the first critical speed by (0,2)*b* mode. Fig. 10(b) shows the imaginary parts of the eigenvalues. The frequency curves in this figure look the same as those of a free spinning disk and an independent oscillating unit. Interaction between the oscillating unit and the disk disappears. The stability boundary is a vertical line at $\bar{\Omega} = 4.35$, and the unstable region lies right to the stability boundary. It means that once there exists a lower damper in the oscillating unit, no matter how small the damping coefficient is, the corresponding backward mode will become negatively damped if the spin rate exceeds the first critical speed. This phenomenon has been reported by Iwan and Moeller [7] and again by Shen and Mote [13]. Consequently, the effect of the lower damper is undesirable to the stability of the whole system although it is favorable to the response of the predominantly oscillating-unit mode. Similar effect can be observed for the upper damper of the oscillating unit.

Fig. 11 depicts the effect of the viscous damping of the disk on the eigenvalues of the whole system. Fig. 11(a) shows the real parts of the eigenvalues. The single curve around the horizontal coordinate axis belongs to the predominantly oscillating-unit mode, and the other curves lying beneath this curve belong to the predominantly disk modes. The three concavities correspond to the intersection of the predominantly oscillating-unit mode and the backward modes, while the other three convexities correspond to the intersection of the predominantly oscillating-unit mode and the reflected modes. The convexities in this case are flatter and wider, while the convexities in the case of an undamped disk (e.g., Fig. 4) are sharper and narrower. These convexities are the unstable intervals. Fig. 11(b) shows the imaginary parts of the eigenvalues. Again the frequency curves in this figure look the same as those of a free spinning disk and the independent oscillating unit. Fig. 12 illustrates the stability boundaries of this problem. There are two large unstable regions and some very small unstable regions. These small unstable regions are formed by the instability of the predominantly disk modes only and will disappear as the damping of the disk increases. However, one of the two large unstable regions is formed by the unstable region of the flutter-type instability between the $(0,3)r$ and the predominantly oscillating-unit modes and the unstable region of the flutter-type instability of the $(0,4)r$ and the predominantly oscillating-unit modes connecting together. The other large unstable region is formed by the flutter-type instability between the $(0,2)r$ mode and the predominantly oscillating-unit mode. The sizes of these two large unstable regions are independent of the damping coefficient of the disk. Therefore,

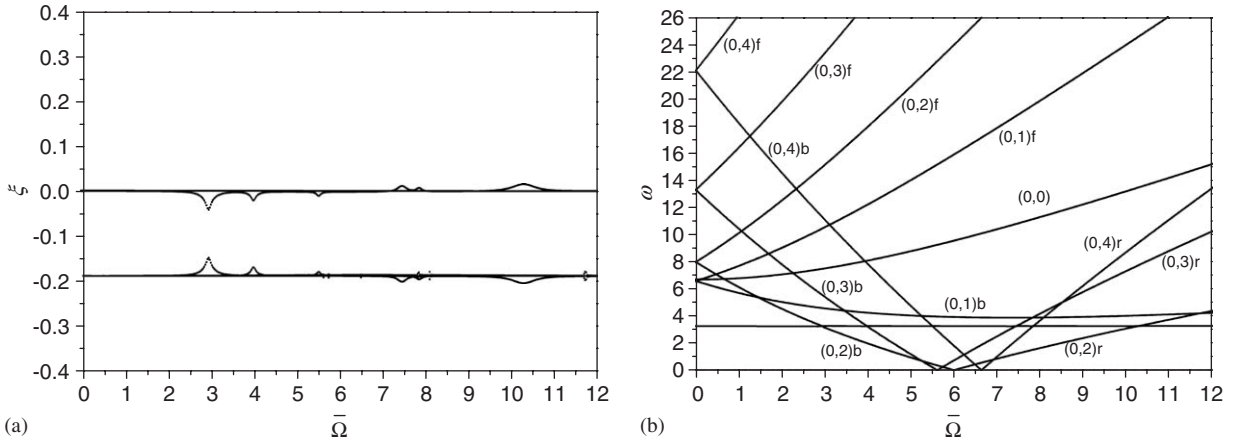

Fig. 11. The real and imaginary parts of the eigenvalues of a damped spinning disk under a stationary oscillating unit. $v = 0.3$, $a/b = 0.3$, $\bar{c} = 0.05$, $\bar{r}_P = 0.7$, $\bar{m}_o = 0.1$, $\bar{k}_P = 0.025$, $\bar{k}_S = 0.05$, $\bar{c}_P = \bar{c}_S = 0$.

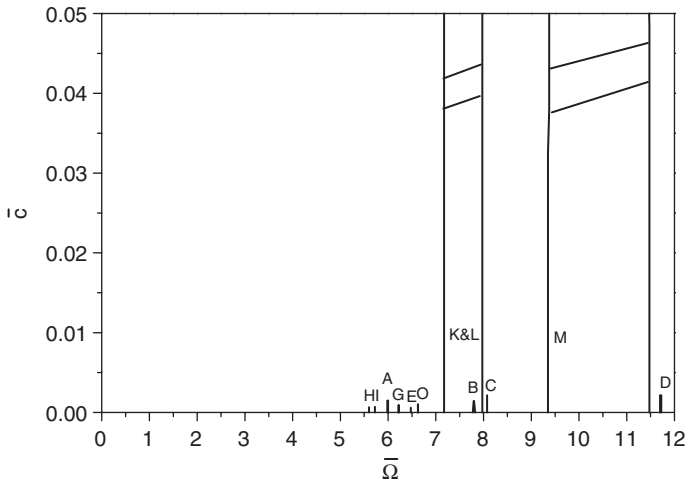

Fig. 12. The stability boundaries of a damped spinning disk under a stationary oscillating unit. $v = 0.3$, $a/b = 0.3$, $\bar{r}_P = 0.7$, $\bar{m}_o = 0.1$, $\bar{k}_P = 0.025$, $\bar{k}_S = 0.05$, $\bar{c}_P = \bar{c}_S = 0$.

the effect of the viscous damping of the disk depresses the unstable regions by the predominantly disk modes only but is unfavorable to the flutter-type instability by the predominantly oscillating-unit mode and the reflected modes.

4. Conclusions

The free vibration and elastic stability of a spinning annular plate transversely in contact with a stationary oscillating unit is studied in this work. The oscillating unit consists of two parallel combinations of springs and dampers attached above and under a mass such that the displacement of the mass is not the same as that of the disk at the contact point. Parametric studies of the system parameters on the stability of the whole system—the disk and the oscillating unit—are conducted in this work. The following conclusions can be drawn:

(1) If the inner radius is assumed to approach zero, and the spring constant and viscous damping coefficient of the lower spring-damper combination are assumed to approach infinity such that the displacement of the

mass is the same as that of the disk at the contact point, the problem considered in this work is reduced to that studied by Iwan and Moeller [7]. Numerical results in this work are identical to those in Iwan and Moeller's paper.

(2) Inclusion of the stiffness between the disk and the mass of the oscillating unit may bring about new and larger unstable regions between the predominantly oscillating-unit mode and the reflected modes but repress the original instability purely by the predominantly disk modes.

(3) The effect of the mass of the oscillating unit is insignificant to the widths of all unstable regions of the whole system but will make the unstable regions of the flutter-type instability between the predominantly oscillating-unit mode and the reflected modes lean toward the lower speed range.

(4) An increase in the spring constant of either the lower spring or the upper spring of the oscillating unit will enlarge all unstable regions of the whole system, and the unstable regions of the flutter-type instability between the reflected modes and the predominantly oscillating-unit mode will lean toward the higher speed range.

(5) Existence of either the lower damper or the upper damper in the oscillating unit will make the backward mode to become negatively damped once the spin rate exceeds the first critical speed but will increase the damping of the predominantly oscillating-unit mode.

(6) The effect of the viscous damping of the disk will depress the unstable regions by the predominantly disk modes only but is unfavorable to the flutter-type instability by the predominantly oscillating-unit mode and reflected modes.

References

[1] H. Lamb, R.V. Southwell, The vibrations of a spinning disk, *Proceedings of the Royal Society* 99 (1921) 272–280.
[2] R.V. Southwell, On the free transverse vibrations of a uniform circular disk clamped at its center and on the effects of rotation, *Proceedings of the Royal Society* 101 (1921) 133–153.
[3] S. Barasch, Y. Chen, On the vibration of a rotating disk, *Journal of Applied Mechanics* 39 (1972) 1143–1144.
[4] S.A. Tobias, Free undamped nonlinear vibrations of imperfect circular disks, *Proceedings of Institute of Mechanical Engineers* 171 (1957) 691–701.
[5] J.L. Nowinski, Nonlinear transverse vibrations of a spinning disk, *Journal of Applied Mechanics* 31 (1964) 72–78.
[6] W.D. Iwan, K.J. Stahl, The response of an elastic disk with a moving mass system, *Journal of Applied Mechanics* 40 (1973) 445–451.
[7] W.D. Iwan, T.L. Moeller, The stability of a spinning elastic disk with a transverse load system, *Journal of Applied Mechanics* 43 (1976) 485–490.
[8] K. Ono, J.S. Chen, D.B. Bogy, Stability analysis for the head-disk interface in a flexible disk drive, *Journal of Applied Mechanics* 58 (1991) 1005–1014.
[9] J.S. Chen, D.B. Bogy, Mathematical structure of modal interaction in a spinning disk-stationary load system, *Journal of Applied Mechanics* 59 (1992) 390–397.
[10] J.S. Chen, D.B. Bogy, Effects of load parameters on the natural frequencies and stability of a flexible spinning disk with a stationary load system, *Journal of Applied Mechanics* 59 (1992) S230–S235.
[11] S.G. Hutton, S. Chonan, B.F. Lehmann, Dynamic response of a guided circular saw, *Journal of Sound and Vibration* 112 (1987) 527–539.
[12] J. Tian, S.G. Hutton, Self-Excited vibration in flexible rotating disks subjected to various transverse interactive forces: a general approach, *Journal of Applied Mechanics* 66 (1999) 800–805.
[13] I.Y. Shen, C.D. Mote Jr., On the mechanisms of instability of a circular plate under a rotating spring-mass-dashpot system, *Journal of Sound and Vibration* 148 (1991) 307–318.
[14] I.Y. Shen, C.D. Mote Jr., Parametric resonances of an axisymmetric, circular plate subjected to a rotating mass, *Journal of Sound and Vibration* 152 (1992) 573–576.
[15] I.Y. Shen, C.D. Mote Jr., Parametric excitation under multiple excitation parameters: Asymmetric plates under a rotating spring, *International Journal of Solids and Structures* 29 (1992) 1019–1032.
[16] S.P. Timoshenko, J.N. Goodier, *Theory of Elasticity*, McGraw-Hill Book Company, New York, 1970.